

Implementation of PV Based Multilevel Inverter to Improve Power Quality using Fuzzy PI and PSO PI Controllers

Ch. Santosh Kumar^{1*} and S. Tara Kalyani²

¹EEE Dept, BVRITH, Hyderabad, India

²EEE Dept, JNTUH, Hyderabad, India

*Correspondence: Ch. Santosh Kumar; chksantosh@yahoo.com

ABSTRACT- Power quality is the primary issue to be taken into consideration in modern electrical systems, particularly on the distribution side, to protect sensitive loads. Long-term uses can never run out of renewable resources. Connecting STATCOM at the distribution side enhances the power factor by improving the quality of the current waveform. The reactive power range that needs adjustment by utilising PV arrays on the STATCOM's DC side. Increases due to the large rise in terms of the PV power plants' size and capacity. Cascaded H Bridge multilevel topologies can increase the flexibility and effectiveness of PV modules. The suggested approach in this paper gives outcome of reduced peak over shoot, rise time, settling time, steady state error, percentage of ripples and total harmonic distortion which improves the power quality. PV system with cascaded H bridge multilevel inverters STATCOM for harmonic suppression and to make reactive powerless. To produce modulation indices for H Bridge switching, synchronised reference frame theory is modified. H bridges' average DC voltage is managed by a PI controller, and controller gains are obtained using fuzzy, PSO, and the trial-and-error approach. To confirm the viability of the suggested approach, simulation results using MATLAB/SIMULINK are shown. The experimental setup of proposed method is carried out to validate the inverter response.

Keywords: Distribution Systems, Fuzzy, Multilevel Inverter, Modulation Index, Power Quality, PI, PSO, STATCOM.

ARTICLE INFORMATION

Author(s): Ch. Santosh Kumar and S. Tara Kalyani;

Received: 05/05/2023; **Accepted:** 01/06/2023; **Published:** 10/06/2023;

e-ISSN: 2347-470X;

Paper Id: IJEER 0505-05;

Citation: 10.37391/IJEER.110219

Webpage-link:

<https://ijeer.forexjournal.co.in/archive/volume-11/ijeer-110219.html>

Publisher's Note: FOREX Publication stays neutral with regard to Jurisdictional claims in Published maps and institutional affiliations.



1. INTRODUCTION

Due to demand for industries and electronic devices, reactive linear loads and nonlinear loads are increasing. Nonlinear loads which uses switching converters require more reactive current and injects harmonics into grid source. This will affect other loads connected to source and also increases the line losses because of poor power factor. To find solutions for these Researchers are always researching on power quality issues such system imbalance, reactive current, load balancing, and harmonics distortion [1]. Initially passive filters are considered for harmonics reduction and for reactive power support. But passive filters are not dynamic and size cost and rating of filters should be increased with increase in power demand. Efficiency and performance of the system will be decreased with increase in amount of harmonics and amount of reactive current in the line [2].

STATCOM which can be connected in shunt at PCC, will improve transient stability and also provides reactive and active power demand and voltage support. STATCOM connected at

distribution line works as active power filters by reducing harmonics and by improving power factor. By connecting renewable energy sources like PV at DC side of the compensator, required amount of reactive power can be injected or absorbed [3].

For high power rating distribution systems, compensators with two or three level inverters for photovoltaic systems are not suitable. The cascaded H Bridge converter for PVSTATCOM is new configuration used which improves dynamic compensation and can capable of overload. Comparing with H Bridge converters with cascaded diode clamped and flying capacitor multilevel inverters require less components [4]. Isolated DC sources are required for each H Bridge, which can be fulfilled by PV array strings. Due to independent DC links to each H Bridge, individual regulation of dc voltage is possible. Generating maximum power from each PV cell can be achieved by using buck boost converter at DC side of each H Bridge. Buck boost converter will regulate output voltage by transforming maximum and constant output power from PV arrays [5].

Synchronous reference frame theory (SRF) can be used to generate switching pulses for STATCOM inverter to compensate the reactive power and to reduce current harmonics [6]. Cascaded voltage and current strategy is proposed in [7] for interface converter. Sequence components control scheme proposed in [8] for CHB based STATCOM. Even when voltage of grid is imbalanced, the voltage of DC link can be adjusted by keeping an eye on the sequence components [9]. However main challenges associated with cascaded H bridge-based PV STATCOM are dynamic stability, balanced and regulated DC voltages and power mismatches of PV array. PV power

mismatches lead to unbalanced power from three phase CHB inverter which will make grid current to be unbalanced. This can be rectified by modifying modulation index using unbalanced factor of power in three phases [10]. Dynamic stability can be improved by making DC voltage to be constant and regulated. PI controller can able to reduce the error between required DC voltage and actual DC voltage only by choosing optimized K_p and K_i gains for controlling. In this paper three tuning methods are adapted to find K_p and K_i gains to regulate DC voltage for better dynamic stability. Seven level H Bridge inverter with SRF controlling is chosen for reducing the harmonics at PCC and for reactive power compensation.

Rest of the paper is prepared which given as: System chosen and description explained in *section II*. Proposed control method with modulation compensation and SRF control theory is explained in *section III*. *Section IV* derives a PV model. *Section V* and *VI* introduced fuzzy adaptive PI controller and

PSO based PI controller for the system with CHB based compensator. *Section VII* explained about interleaved DC buck boost converter. *Section VIII* presents simulation results to check effectiveness of proposed control system.

2. SYSTEM DESCRIPTION

Static compensator using *figure 1* depicts a CHB multilevel inverter with PV with DC side for improved power quality. For seven level, Three H Bridge converter connected together series to generate seven levels ($-3V_{dc}, -2V_{dc}, -V_{dc}, 0, V_{dc}, 2V_{dc}, 3V_{dc}$) which are required to get seven level output voltage. DC link voltage for each converter is supplied through a DC-to-DC converter from a series of PV panels. Switching harmonics in injected voltage and currents can be reduced by LC filter through which seven level structure is connected to PCC. H module is shown in *figure 2*.

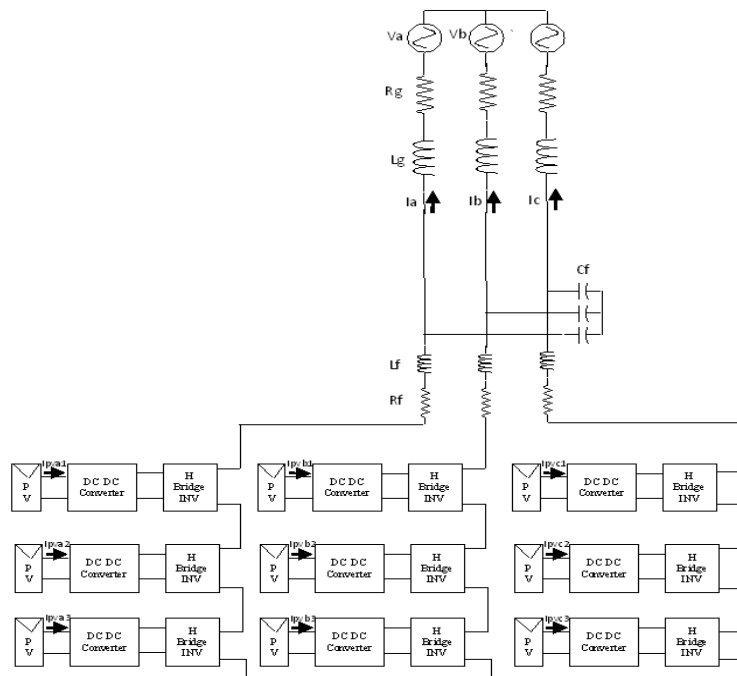


Figure 1: Cascaded H Bridge seven level inverter with PV at DC side

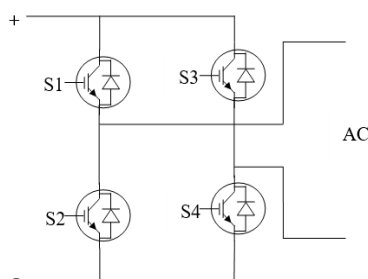


Figure 2: H Bridge Module

Depending on the switching pulses applied to H Bridge, it generates three output voltage levels $-V_{dc}, 0, +V_{dc}$. For series connected n modules, $2n + 1$ voltage levels can be generated. As, for better harmonic compensation and for smooth current

waveform, seven level is considered in this paper. Because of increased levels in voltage waveform, synthesized current is free of harmonics and requirement of more rated output filters can be reduced. Due to increased number of levels voltage stress on each switch can be reduced and hence efficiency will be improved compared to other topologies. For seven level converter 3 H Bridge modules should be connected in series for each phase and connected to PCC through filter. By applying KVL to one phase of the compensator

$$\sum_{j=1}^n v_j - v_g - R_f i_g - L_f \frac{di_g}{dt} = 0 \quad (1)$$

Here v_j is voltage output came by j^{th} module, L_f is the filter inductance, R_f is the resistance of the filter, n is number of H bridges, v_g is voltage grid and i_g is current in grid.

By applying KCL at DC node

$$I_{Cj} + C_f \frac{dv_{cj}}{dt} = 0, (j = 1, \dots, n) \quad (2)$$

Where C_f the capacitance of filter is, V_{cj} is the voltage across individual capacitors and I_{Cj} is current flowing into j th capacitor. Power on the both side of the converter are equivalent when switching losses are ignored.

$$I_{Cj} = \frac{v_j}{v_{cj}} i_g \quad (3)$$

$$\frac{v_j}{v_{cj}} i_g + C_f \frac{dv_{cj}}{dt} = 0 \quad (4)$$

from equation (1)-(4) generated voltage output of converter can control grid current, modifying component(active) of the generated voltage output can balance individual capacitor voltages.

For each H Bridge of multilevel inverter, a dedicated DC source is required to maintain constant and regulated DC voltage, to get required levels at AC side. Feasibility of independent voltage control is possible because of separate DC links. This can be achieved by connecting PV array to each H Bridge

through DC-to-DC buck boost converter at DC side. DC to DC converter regulates the PV voltage and maintain constant and reduced ripple voltage at DC side of H Bridge. Interleaved buck boost converter is chosen to get better regulation in DC voltage [11-14]. PV array model is presented in section IV. Controllers and optimization is discussed in section VI and VII.

3. PROPOSED CONTROL METHOD

For Cascaded H Bridge seven level inverter, an advanced control method should be used to improve grid currents quality and to compensate reactive power. Current sine wave which is distorted due to harmonics injected by non-linear loads can be corrected or improved by injecting harmonics current in negative polarity with grid currents. Improvement of current wave also leads to reduction of distortions in voltage waveform. Reactive power burden on grid due to inductive loads can be reduced by injecting reactive current required by load into PCC by seven level H Bridge inverter. Hence, this will improve the power factor at source side and will reduce losses withstanding by other loads. These are the objectives to be consider while choosing a control method. Hence, an advanced SRF based control method is used and schematic is shown in figure 3.

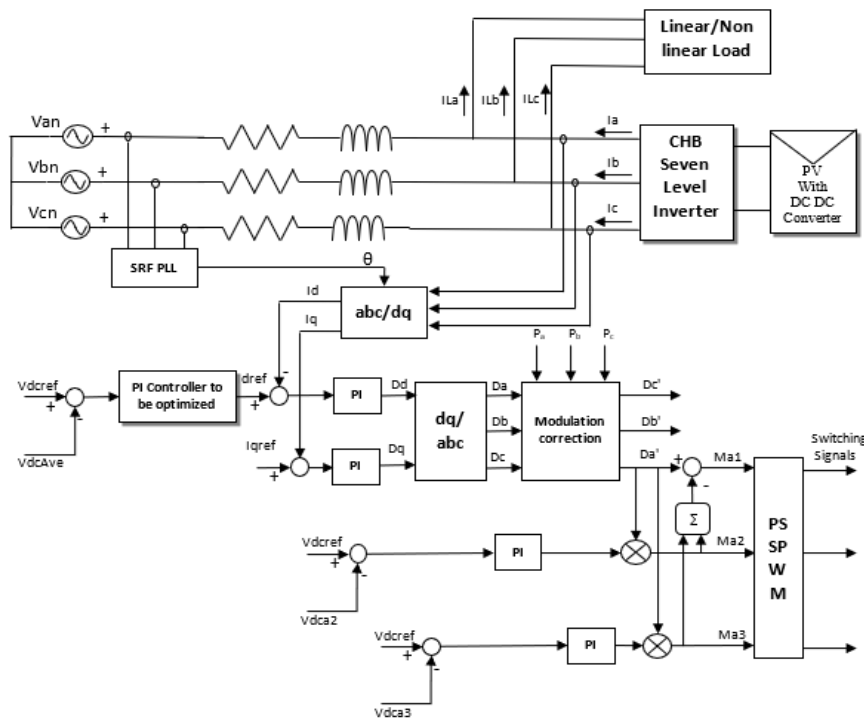


Figure 3: Control Scheme CHB Multilevel inverter

3.1 SRF Control

DQ control or SRF control which is applied to H bridge reactive power compensation and inverter for harmonics is having two loops. One is DC outer voltage regulation loop and another one is current inner control loop. Outer voltage loop regulates average DC voltage of 9 H Bridge inverters and inner current loop is compensating current harmonics and reactive power. Three phase voltages and current are transformed in x to dq0 components using parks transformation.

$$\begin{bmatrix} X_d \\ X_q \\ X_0 \end{bmatrix} = \sqrt{\frac{2}{3}} \begin{bmatrix} \sin \theta & \sin \left(\theta - \frac{2\pi}{3} \right) & \sin \left(\theta + \frac{2\pi}{3} \right) \\ \cos \theta & \cos \left(\theta - \frac{2\pi}{3} \right) & \cos \left(\theta + \frac{2\pi}{3} \right) \\ \frac{1}{\sqrt{2}} & \frac{1}{\sqrt{2}} & \frac{1}{\sqrt{2}} \end{bmatrix} \begin{bmatrix} X_A \\ X_B \\ X_C \end{bmatrix} \quad (5)$$

Where X is either voltage V or current I and θ is phase of grid voltage.

Reference value for direct axis current $I_{d_{ref}}$ is determined from PI controller which regulates average DC voltage of H bridges. Average of 9 H Bridges DC voltages is compared to voltage reference and PI controller is used to reduce tracking error and to improve dynamic behavior. In this paper, two algorithms fuzzy PID and PSO PID are considered for tuning of the PI controller. These two algorithms are explained in next sections. $I_{q_{ref}}$ can be set as zero and in case of reactive power compensation reactive current can be calculated using load reactive current requirement. $I_{d_{ref}}$ and $I_{q_{ref}}$ are compared to actual I_d and I_q using PI controllers which are tuned using trial and error method. Output of PI controllers are modulation indices D_a, D_q in DQ frame and these are transformed into three phase D_a, D_b, D_c using inverse parks transformation.

$$\begin{bmatrix} X_A \\ X_B \\ X_C \end{bmatrix} = \sqrt{\frac{2}{3}} \begin{bmatrix} \cos \theta & -\sin \theta & \frac{1}{\sqrt{2}} \\ \cos \left(\theta - \frac{2\pi}{3} \right) & -\sin \left(\theta - \frac{2\pi}{3} \right) & \frac{1}{\sqrt{2}} \\ \cos \left(\theta + \frac{2\pi}{3} \right) & -\sin \left(\theta + \frac{2\pi}{3} \right) & \frac{1}{\sqrt{2}} \end{bmatrix} \begin{bmatrix} X_d \\ X_q \\ X_0 \end{bmatrix} \quad (6)$$

In addition, with average DC voltage controlling, individual voltage control is required for each H Bridge to make PV module works at maximum power point. Consider phase A, two separate voltage loops with PI controller is used to generate modulation index proportions ($Sa2, Sa3$). These values can be multiplied with modulation index of phase A (D_a) to generate two indices $Ma2, Ma3$ for second and third H bridges. $Ma1$ can be generated by subtracting the sum of $Ma2, Ma3$ from D_a . By using phase shifted SPWM (PSSPWM) pulses are generated for seven level output voltage [15-18]. Same process of pulse generation can be applied to phase B and phase C.

3.2 Modulation Correction

Due to atmospheric conditions PV arrays connected H bridges may not generate equal powers which lead to severe problems in H Bridge cascaded multilevel inverter. There is a possibility of unbalanced currents into the grid because of power mismatches in PV array connected to each H bridge module. To rectify this problem, modulation index can be corrected to make output phase voltage to be in proportional to the unbalanced power and thereby make currents to be balanced. Modification of modulation index imposes zero sequence voltage into each phase to make currents to be balanced.

Weighted ratio of unbalanced power r_j is calculated as

$$r_j = \frac{P_{inav}}{P_{inj}} \quad (7)$$

Where P_{inj} is the power input of phase j ($j = A, B, C$), P_{inav} average power of three phases.

Then the modulation index correction to impose zero sequence voltage is given as

$$D_o = \frac{1}{2} [\min(r_a \cdot D_a, r_b \cdot D_b, r_c \cdot D_c) + \max(r_a \cdot D_a, r_b \cdot D_b, r_c \cdot D_c)] \quad (8)$$

Where D_a, D_b, D_c are the modulation indices determined by current loop controller.

After the correction modulation index of each phase can be updated as

$$\begin{aligned} D'_a &= D_a - D_o \\ D'_b &= D_b - D_o \\ D'_c &= D_c - D_o \end{aligned} \quad (9)$$

4. PV ARRAY MODEL

Power generation of PV cell and its operation characteristics are affected by many environmental factors. Solar irradiance G , in W/m^2 , temperature t in $^{\circ}C$ are two main factors to be considered while defining of PV characteristics of cell. Characteristics I-V and P-V of PV system varies with the intensity of solar irradiation and cell temperature. To get required output power and voltage solar photovoltaic cells are connected in parallel and series referred as PV modules.

Single diode model shown in figure 4 is mostly used to describe characteristics of PV cell. Parallel shunt resistance R_{sh} consider leakage currents of cell and series resistance R_s consider shading effects of PV cell.

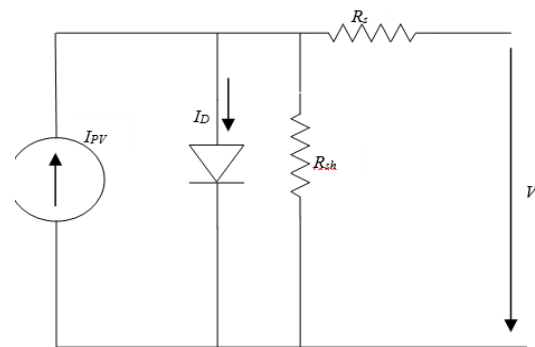


Figure 4: Single diode model of solar cell

Based on semiconductors theory, ideal PV cell's the fundamental equation can be used to define I-V characteristics.

$$I = I_{ph} - I_{sat} \left[\exp \left(\frac{q(V+IR_s)}{kT_C A} \right) - 1 \right] - \frac{(V+IR_s)}{R_{sh}} \quad (10)$$

Where I_{ph} is photocurrent, I_{sat} is the saturation cell current, q is an electron charge ($1.6 \times 10^{-19} C$), k is a Boltzmann's constant ($1.38 \times 10^{-23} J/K$), T_C is the cell's working temperature, A is an ideal factor, R_{sh} is a shunt resistance and R_s is a series resistance. The photocurrent of cell depends on solar insolation, working temperature of cell, given as

$$I_{sat} = I_{Rsat} \left(\frac{T_C}{T_{ref}} \right)^3 \exp \left[\frac{qE_G \left(\frac{1}{T_{ref}} - \frac{1}{T_C} \right)}{kA} \right] \quad (11)$$

Where I_{Rsat} is the reverse saturation current under standard sun illumination & temperature. E_G is the band gap energy of semiconductor used in the cell.

The sun insolation and the cell's working temperature, which is stated as, determine the photo current I_{ph} primarily.

$$I_{ph} = [I_{SC} + K_I(T_C - T_{ref})]G \quad (12)$$

Where T_{ref} is the reference temperature for the cell, G is the solar insolation in kW/m^2 , I_{SC} is the cell's short-circuit current at 25°C and 1 kW/m^2 , K_I is the temperature coefficient of short circuit current, and T_{ref} is the cell's short-circuit current. Typically, a PV cell produce very low voltage and power, When PV cells are arranged in series and parallel to provide the necessary voltage and power, the PV array's current and voltage equation becomes

$$I = N_p I_{ph} - N_p I_{sat} \left[\exp\left(\frac{q\left(\frac{V}{N_s} + IR_s\right)}{kT_C A}\right) - 1 \right] - \frac{(N_p V + IR_s)}{R_{sh}} \quad (13)$$

N_p is the number of parallel PV cells and N_s is the number of series PV cells.

Output I-V and P-V characteristics of PV array are shown in figure 5-8. Figure 5 and 6 showing the variation of current and power respectively under variable solar irradiance and constant temperature. Figure 7 and 8 showing the variation under variable temperature and constant irradiation. From these it is clear that variation of current and hence power with respect to voltage is nonlinear and varying with solar irradiation and temperature. Even during variations in atmospheric conditions, it is necessary to provide maximum power to the load and consequently, solar PV systems should adopt MPPT.

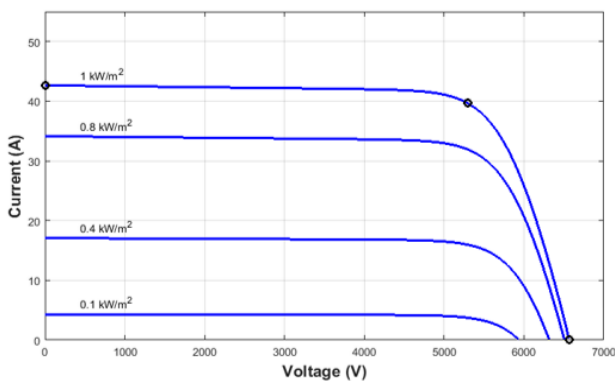


Figure 5: Variation of current with respect to voltage in constant temperature (250°C) and different irradiation levels

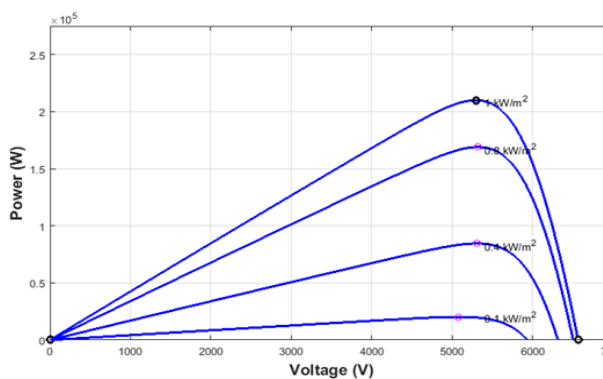


Figure 6: Variation of power with respect to voltage in constant temperature (250°C) and different irradiation levels

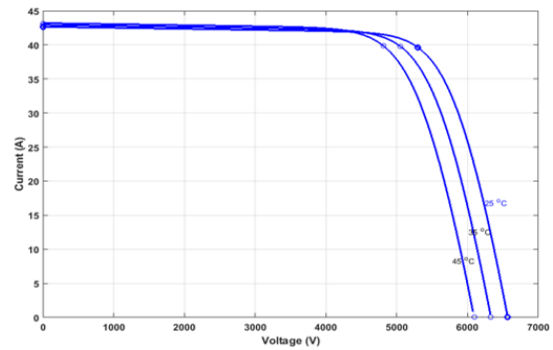


Figure 7: Variation in current to voltage in constant irradiation (1000 W/m^2) and different temperatures

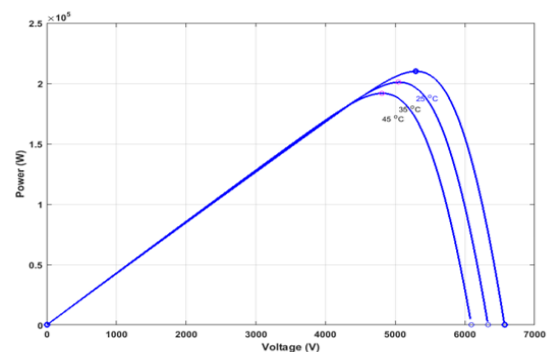


Figure 8: Variation of power with respect to voltage in constant irradiation (1000 W/m^2) and different temperatures

5. FUZZY TUNED ADAPTIVE PI CONTROLLER

For controlling linear systems, conventional PI controller is simple and efficient. But for nonlinear systems such as PV based distribution systems in which control performance deteriorate with working conditions of the system normal PI controller is not effective. PI control with Variable parameters in proportional with working conditions can overcome this problem. Based on variable parameters fuzzy based PI controller can be designed. The detailed structure of the controller in figure 9.

The equation of the adaptive PID fuzzy is

$$u(t) = K_p e(t) + K_i \int [e(t) + Ku_2(t)] \quad (14)$$

$$u_2(t) = u_1(t) - u_0(t) \quad (15)$$

$u(t)$ is the control action, K_p, K_i are proportional and integral gains. $e(t)$ is the tracking error signal.

For fuzzy tuned PI controller input are error e and the change of error ce , given as

$$e(k) = V_{dcref}(k) - V_{dc}(k) \quad (16)$$

$$ce(k) = e(k) - e(k-1) \quad (17)$$

And the outputs of the fuzzy controller are variation in proportion and integral gain. Process of Fuzzy controller includes: fuzzification, rule base and defuzzification.

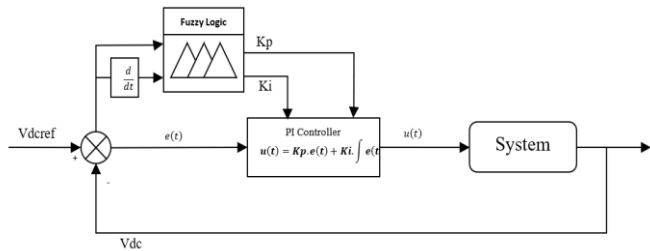


Figure 9: Fuzzy Adaptive PI controller

Fuzzification converts crisp values into linguistic sets by using fuzzy membership functions. Seven fuzzy membership functions are defined here including NB (Negative Big), nm (negative medium), ns (negative small), zo (zero), ps (positive small), pm (positive medium), pb (positive big).

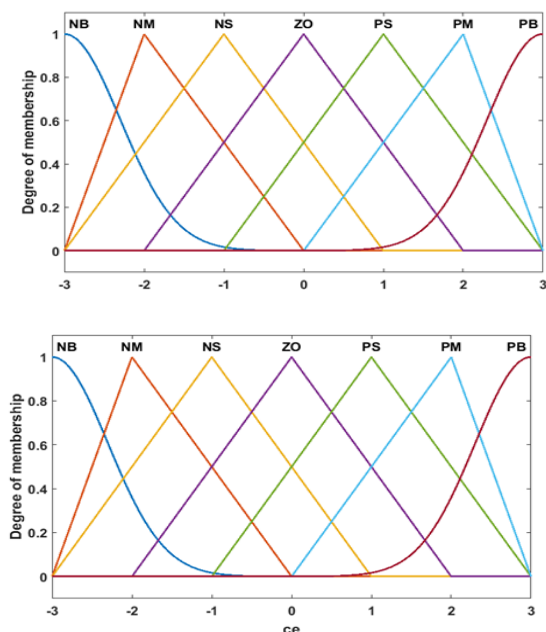


Figure 10: Membership function of input error[e] and change in error (ce)

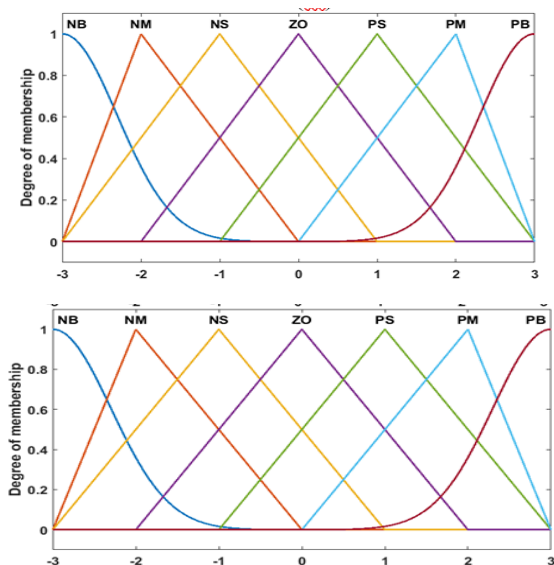


Figure 11: Membership functions of outputs KP and KI

Output of the fuzzy logic controller can be decided by rule base. Mamdani inference method is chosen for this rule base. Membership value of the output is given as

$$\mu_{K_{p1}}(c_p) = \mu_e(e) \wedge \mu_{ec}(ec) \quad (18)$$

$$\mu_{K_{i1}}(c_i) = \mu_e(e) \wedge \mu_{ec}(ec) \quad (19)$$

Rule base comprises of 49 rules to decide the output for 7 membership functions of two inputs. Rules of Fuzzy are shown in table 1-2.

Table 1: Kp Rule base

e \ ce	nb	nm	ns	zo	ps	pm	pb
nb	pb	pb	pm	pm	ps	zo	zo
nm	pb	pb	pm	ps	ps	zo	ns
ns	pm	pm	pm	ps	zo	ns	ns
zo	pm	pm	ps	zo	ns	nm	nm
ps	ps	ps	zo	ns	ns	nm	nm
pm	ps	zo	ns	nm	nm	nm	nb
pb	zo	zo	nm	nm	nm	nb	nb

Table 2: Ki Rule base

e \ ce	nb	nm	ns	zo	ps	pm	pb
nb	nb	nb	nm	nm	ns	zo	zo
nm	nb	nb	nm	ns	ns	zo	zo
ns	nb	nm	ns	ns	zo	ps	ps
zo	nm	nm	ns	zo	ps	pm	pm
ps	nm	ns	zo	ps	ps	pm	pb
pm	zo	zo	ps	ps	pm	pb	pb
pb	zo	zo	ps	pm	pm	pb	pb

In defuzzification output of the fuzzy controller can be determined by weighted mean. Then from the fuzzy output proportional and integral gains are calculated as:

$$K_p = K_{po} + K_1 \cdot K_{p1} \quad (20)$$

$$K_i = K_{io} + K_2 \cdot K_{i1} \quad (21)$$

K_{po} is the initial value of the proportion gain, K_{io} is the initial value of the integral gain. K_1 and K_2 are constants.

6. PARTICLE SWARM OPTIMIZATION

Research communities and industries are increasing their attention on optimization algorithms in the past few years. To find the maximum or the minimum of a function with certain constraints optimization algorithm can be used. In area of designing a fitness function, multimodal optimization technique, parameter control methods computational intelligence which is successor of artificial intelligence is having major role. Compared with traditional optimization methods computational intelligence can find optimum values even in complicated optimization problems [19-21].

One of the efficient optimization techniques in computational intelligence, which is based on swarm intelligence, is Particle Swarm Optimization (PSO). Animal behaviors and their social interaction such as bird flocking and fish schooling are the main motivation for this method. Competition and cooperation among the entire population of birds to find food is used to find optimal solution in PSO. Individual parameters of a swarm represent different possible set of the unknown values to be optimized. Population of some random solutions are set as initialization values of swarm. A multi-dimensional search space and particles flying around that space by adjusting their position and velocity can be defined in PSO systems. The main goal of PSO algorithm is to effectively search the solution space by particle swarming into the best-fitting solution obtained in earlier rounds with the goal of running into better solutions along the way and ultimately settling on a single minimal or maximum solution. Efficiency to find solution to the fitness function will define the performance of each particle to find solution.

In this paper, PSO algorithm is used to obtain optimal PI controller gains for a high-performance DC voltage regulation. Proportionality constant and Integral constant are tuned using possible controller setting of particles to reduce the error function as much as possible. Integral Time of Absolute Error is the error function employed here. In PSO algorithm, particles which are population of random solutions can be assigned to a system as initialization and each solution of these particles is also assigned a randomized velocity. This algorithm depends on information exchange between particles or random solutions. The trajectory of each particle into best solution for fitness function can be adjusted by itself. Trajectory of each particle can be modifying previous position attained by any nearby particle.

The performance of each particle can be evaluated by fitness function by observing whether the best fitting solution is achieved. During the process of algorithm, for every iteration each particle and fitness of the best individual particle improves and moves towards solution and hence to the end of the run [22-25].

At first in PSO algorithm swarm with no. of individuals called as particles are initialized. Every i^{th} particle in swarm holds the information of its position occupied x_i , its moving velocity v_i , the best position which is link with the best fitness value achieved by a particle far $pbest_i$ and the global best position which is link with best fitness value among all the particles $gbest$.

In our application positions of particles represents the gains of PI controller (K_p, K_i). The position of each particle defines fitness of a particle. Particle closure to the solution will have higher fitness value then the particle which far away. For every iteration every particle position and velocity are updated to get better fitness by using the equation:

$$v_{ij}^{t+1} = v_{ij}^t + c_1 \cdot rand_{1j}^t \cdot (pbest_{ij}^t - x_{ij}^t) + c_2 \cdot rand_{2j}^t \cdot (gbest_{ij}^t - x_{ij}^t) \quad (22)$$

$$x_{ij}^{t+1} = x_{ij}^t + v_{ij}^{t+1} \quad (23)$$

For $i = 1, 2, \dots, n$ where n is the number of particles, $j = (1, 2, \dots, d)$ as d is number of dimensions, t is the iteration number, w is the inertia weight, $rand1$ and $rand2$ are 2 random numbers distributed uniformly in the range $[0, 1]$, $c1$ and $c2$ are the acceleration factors. $c1$ is cognitive acceleration constant, forces the particle to move into the position to get the more fitness and $c2$ is social acceleration constant forces the particle towards the particle that currently has highest fitness.

Velocity of particle should be bounded between chosen limits $v_{min} < v_{id} < v_{max}$ and particle position is also bounded as $x_{min} < x_{id} < x_{max}$. The personal best of each particle can be updated as

$$pbest_i^{t+1} = \begin{cases} pbest_i^t, & \text{if } f(pbest_i^t) < f(x_i^{t+1}) \\ x_i^{t+1}, & \text{if } f(pbest_i^t) > f(x_i^{t+1}) \end{cases} \quad (24)$$

Then the global best of swarm can be updated as:

$$gbest^{t+1} = argmin. f(pbest_i^{t+1}) \quad (25)$$

f is a function to evaluate fitness value of given position.

This process of PSO can be repeated iteratively until maximum iterations are reached or no improvement over a number of iterations. PSO algorithm Flow chart is shown in figure 12.

To evaluate the performance of the PID controller different indices are used such as integral of absolute error (IAE), Integral of Squared Error (ISE), Integral of Time Squared Error (ITSE) and Integral of Time Absolute Error (ITAE).

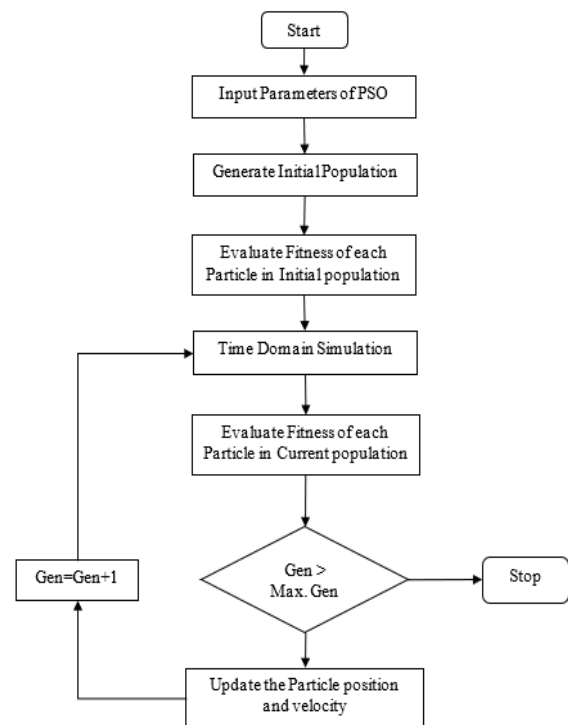


Figure 12: Flow chart of PSO algorithm

These indices will define the minimization of error signal given as the input to PI controller. In this work ITAE is used as fitness function for PSO to tune the PI gains.

$$ITAE = \int_0^{\infty} t|e(t)| dt \tag{26}$$

$$e(t) = V_{dcref}(t) - V_{dc}(t) \tag{27}$$

7. SIMULATION RESULTS

To exhibit the performance of proposed control strategy the system shown in *figure 13* is simulated using MATLAB/SIMULINK using tools simscape, Fuzzy logic and PSO. System Parameters used in simulation are given in *table 3*. PI controllers are tuned using trial and error, fuzzy and PSO. These three tuning methods are compared to check tracking

behavior of DC voltage across H Bridge DC side and results are tabulated.

Seven level H bridge inverter connected to grid for harmonics reduction and reactive power compensation is simulated and tested. Each H Bridge is connected to its dedicated solar array through DC-DC buck-boost converter. Inverter is connected to PCC through RLC filter to smooth stepped voltage and current waveforms. 210 KW PV panel with 185 series modules and 5 parallel strings are connected to H Bridge. In detailed parameters of PV panel are given in table. High reactive linear load, non-linear load are considered to check effectiveness of fuzzy and PSO tuned PID controller for dynamic stability. Simulated system in MATLAB environment is shown in *figure 14*. Seven level CHB multilevel converter is shown in *figure 15*.

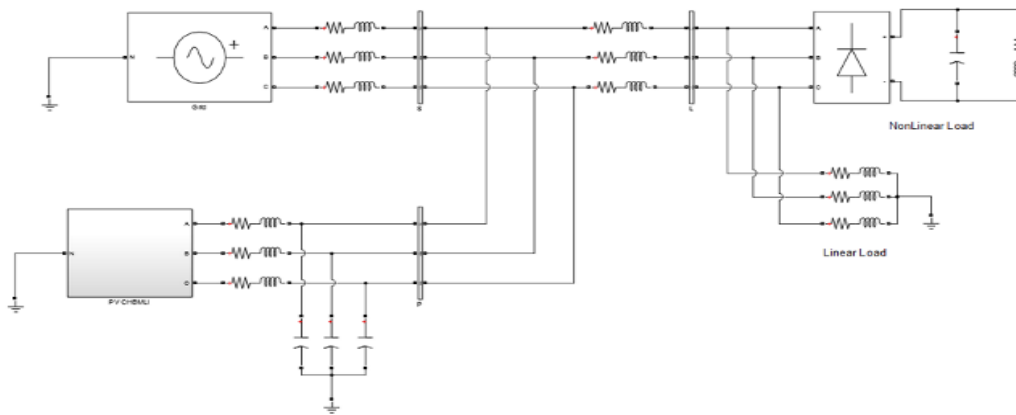


Figure 13: System simulated with PVCHBMLI as compensator and with Linear and Non-linear Load

Table 3: Parameters of the System

PV	
Voltage (Open Circuit) (Voc):	35.5 V
Current (Short Circuit) (Isc):	8.52 A
Voltage at maximum power point Vmp	28.63 V
Current at maximum power point Imp	7.93 V
Series connected modules per string Ns:	185
Parallel strings Np:	5
Grid	
Grid Voltage:	11 KV
Frequency:	50 Hz
Resistance Rg:	0.5 Ω
Inductance Lg:	2.9 mH

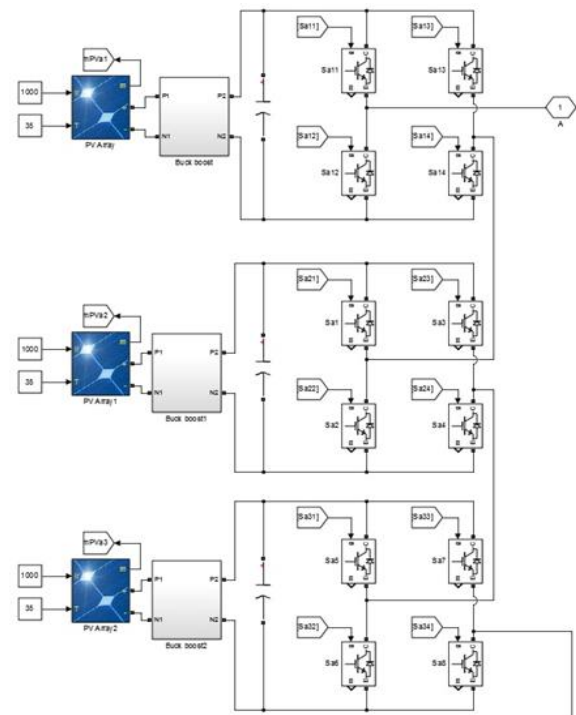


Figure 14: 7 level Cascaded H bridge converter of A Phase with PV and buck boost converter

7.1 DC Voltage Regulation

PI controller is used to regulate average DC side voltages of 9 H Bridges to track the reference value and to improve dynamic stability. Three tuning methods are adopted to determine PI control gains. A simple trial and error method which uses the technique of guess and check, fuzzy tuned PI controller in which PI controller gains can be determined by fuzzy by taking error and change in error as inputs and PSO based PID in which PI controller gains can be optimized by particle swarm optimization using Integral time absolute error (ITAE) as fitness function. Average DC voltage regulated using these three tuning methods are shown in *figure 16*. to check performance of these three tuning methods, peak over shoot, rise time, settling time, steady state error and percentage of ripples are tabulated in *table 4*. In which clearly shows that PSO based PI tuning is good among three.

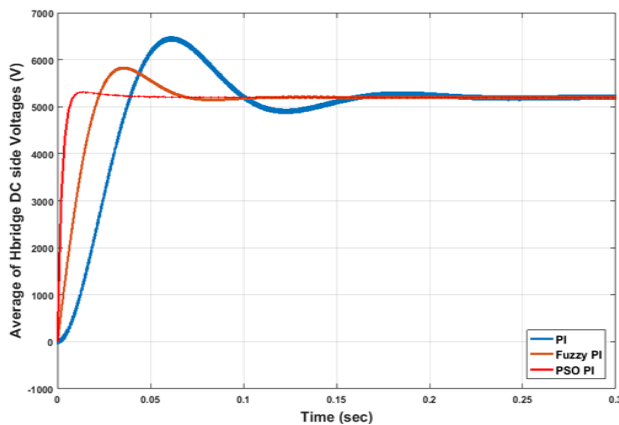


Figure 15: Average of 9 H Bridge DC side voltages regulated by PI, Fuzzy PI and PSO PI controllers

Table 4: PI controller performance to regulate DC side voltage of H Bridge

Controller	Peak Overshoot	Settling Time	Rise Time	Steady State Error	Ripples
PI	24.9%	0.290	0.0388	2.56	1.07%
Fuzzy PI	12.51%	0.125	0.02182	1.21	0.5%
PSO PI	2.24%	0.08	0.00847	0.25	0.0999%

7.2 Nonlinear Load

Source is coupled to nonlinear load of uncontrolled diode bridge rectifier with RL load of 50, 100mH. Due to switching transients of diode, harmonics can be introduced into source current. These harmonics are filtered by Cascaded H bridge converter by injecting negative harmonics into PCC. The same climatic conditions apply to all PV panels, with an irradiation of 1000 W/m² and a temperature of 25 °C. Seven level H bridge inverter output voltage before and after filter are shown in *figure 16-17*. Due to large number of reduced ripples in DC voltage for PSO based PI technique, source current is almost harmonics free with very less amount of Total Harmonic Distortion (THD). THD values for three methods are tabulated in *table 5*.

Table 5: Total harmonic distortion of source and load currents, for nonlinear and linear loads, with three controllers

	Non-linear Load (%)	Linear and non-linear Load (%)
Load Current THD	28.84	19.44
PI	5.36	4.1
Fuzzy based PI	2.8	2.06
PSO Tuned PI	1.36	0.99

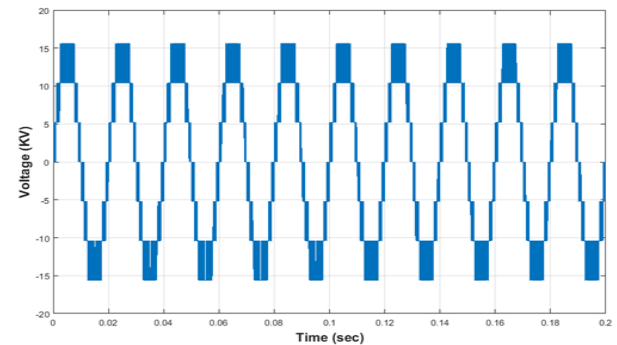


Figure 16: 7 level-H bridge inverter output voltage before filter

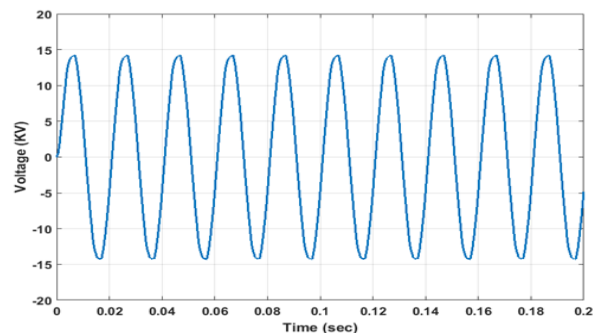


Figure 17: 7 level- H bridge inverter output voltage after filter

8. EXPERIMENTAL RESULTS

The proposed method is done in simulation and also an experimental prototype is implemented to confirm the simulation results which is as shown in *figure 18*, control signals are shown in *figure 19* and *figure 20* and output voltage in *figure 21*. Sinusoidal pulse width modulation is used to generate control signals for switching power switches. The output voltage of inverter is successfully produced and filtered to get sine wave which results lesser total harmonic distortion and results meets with simulation results.

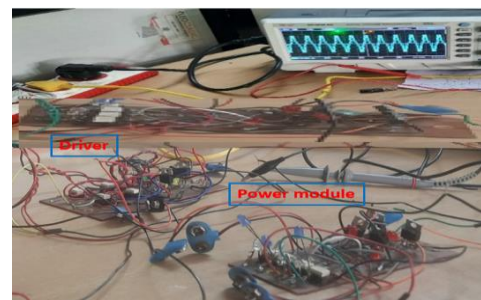
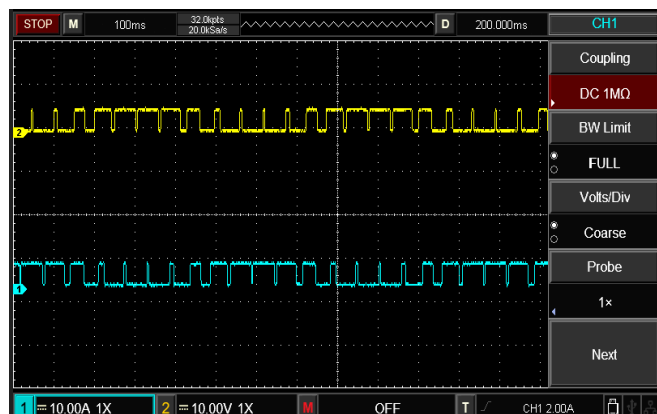
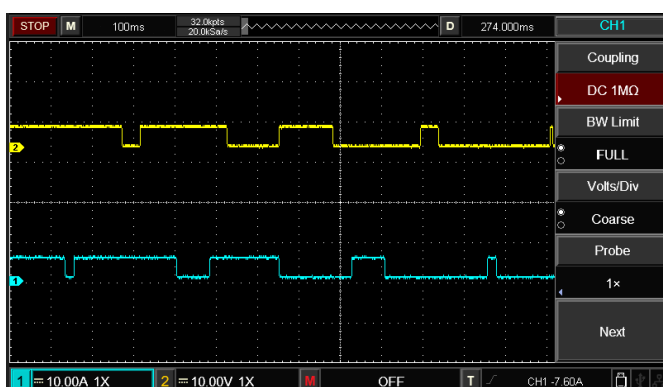
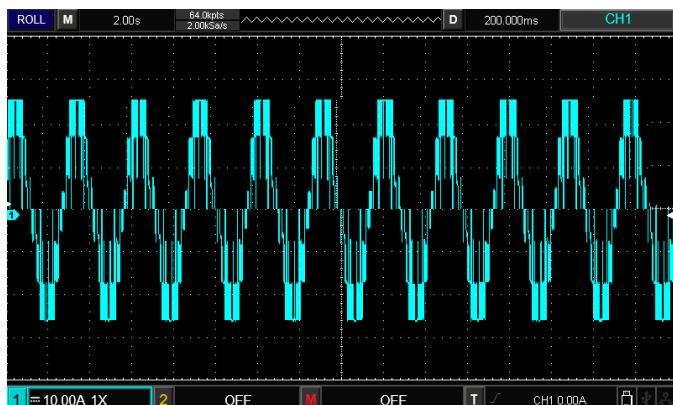


Figure 18: Experimental Setup


Figure 19: Control Signals

Figure 20: Control Signals

Figure 21: Output Voltage

9. CONCLUSION

This research presents a cascaded H-bridge 7 level inverter-based PV STATCOM to adjust reactive power and harmonics reduction at PCC. Individual PV arrays are connected to each H Bridge at DC side through interleaved buck boost converter for constant and maximum power extraction. To produce modulation indices for H Bridge switching, synchronised reference frame theory is modified. To rectify power mismatches in PV arrays, which leads to unbalanced grid currents, modulation indices are modified by adding a value called modulation compensation. H bridges' average DC voltage is managed by a PI controller, and controller gains are

fine-tuned using the trial and error, fuzzy, and PSO methods. Simulation results are presented by using these three tuning methods. In dc voltage with PSO based PI controller tracking error, peak overshoot and percentage of ripples are very less compared to other two methods. The results of inverter output are experimentally confirmed and hence CHB seven level inverter-based PV STATCOM with PSO tuned PI controller is efficiently improves the power quality by increasing quality of current waveform at source side of the line.

List of Abbreviations

STATCOM	Static Synchronous Compensator
PV	Photo Voltaic
CHB	Cascaded H Bridge
PSO	Particle Swarm Optimization
PCC	Point of Common Coupling
SRF	Synchronous Reference Frame

REFERENCES

- [1] Beres, R.N.; Wang, X.; Liserre, M.; Blaabjerg, F.; Bak, C.L. A review of passive power filters for three-phase grid connected voltage-source converters. *IEEE J. Emerg. Sel. Top. Power Electron.* 2016, 4, 54–69
- [2] Prakash Mahela, O.; Gafoor Shaik, A. Topological aspects of power quality improvement techniques: A comprehensive overview. *Renew. Sustain. Energy Rev.* 2016, 58, 1129–1142.
- [3] Junbiao, H.; Solanki, S.K.; Solanki, J.; Schoene, J. Study of unified control of STATCOM to resolve the Power quality issues of a grid-connected three phase PV system. In *Proceedings of the 2012 IEEE PES Innovative Smart Grid Technologies (ISGT)*, Washington, DC, USA, 16–20 January 2012; pp. 1–7.
- [4] De León Morales, J.; Mata-Jiménez, M.T.; Escalante, M.F. Adaptive scheme for DC voltages estimation in a cascaded H-bridge multilevel converter. *Electr. Power Syst. Res.* 2011, 81, 1943–1951.
- [5] Mohamed Kaouane, Akkila Boukhelifa, Ahmed Cheriti, 'Regulated output voltage double switch buck-boost converter for photovoltaic systems', *International journal of hydrogen energy*, Volume 41, Issue 45, 2016, 20847-20857.
- [6] Donghua, C.; Shaojun, X. Review of the control strategies applied to active power filters. In *Proceedings of the 2004 IEEE International Conference on Electric Utility Deregulation, Restructuring and Power Technologies*, Hong Kong, China, 5–8 April 2004; Volume 2, pp. 666–670.
- [7] Qing-Chnag Zhong, Tomas Hornik, 'Cascaded Current-Voltage control to improve the power quality for a grid connected inverter with a local load' *IEEE Transactions on Industrial Electronics*, Volume 60, Issue 4, 2013, 1344-1355.
- [8] Nobuhiko Hatano, Toshifumi Ise, 'Control scheme of cascaded H-Bridge STATCOM using zero sequence voltage and negative sequence current' *IEEE Transactions on Power Delivery*, Volume 25, Issue 2, 2010, 543-550
- [9] Camacho, A.; Castilla, M.; Miret, J.; Vicuña, L.G.d.; Guzman, R. Positive and Negative Sequence Control Strategies to Maximize the Voltage Support in Resistive-Inductive Grids During Grid Faults. *IEEE Trans. Power Electron.* 2018, 33, 5362–5373.
- [10] G. Farivar, B.Hredzak, V.G.Agelidis, 'Decoupled control system for cascaded H-Bridge Multilevel Inverter based STATCOM' *IEEE Transactions on Industrial Electronics*, Volume 63, Issue 1, 2016, 322-331
- [11] Fei Yang, Xinbo Ruan, Gang Wu, Zhihong Ye, 'Discontinuous current mode operation of Two-phase interleaved DC-DC converter with coupled inductor', *IEEE Transactions on Power Electronics*, Volume 33, Issue 1, 2018, 188-198

- [12] T.Bartz–Beielstein K.E. Parsopoulos and M.N. Vrahatis, “Analysis of Particle Swarm Optimization Using Computational Statistics”, International conference on numerical analysis and applied mathematics ICNAAM (2004).
- [13] Thomas Beielstein, K.E. Parsopoulos and Michael N. Vrahatis , “Tuning PSO Parameters Through Sensitivity Analysis, Technical Report of the Collaborative Research Center 531 Computational Intelligence CI–124/02, University of Dortmund, January (2002).
- [14] RohitRamachandran, S.Lakshminarayanan and G.P Rangaiah”Process identification using open-loop and closed loop step responses”Journal of the institute of Engineers,Singapore vol.45,Issue6 (2005).
- [15] Hajar Chadli1 , Sara Chadli2 , Mohamed Boutouba3 , Mohammed Saber4 , Abdelwahed Tahani5 “Hardware implementation and performance evaluation of microcontroller-based 7-level inverter using POD-SPWM technique” Indonesian Journal of Electrical Engineering and Computer Science Vol. 23, No. 1, July 2021
- [16] Abdullayev V, Bhadouria RP. Overview of the Conversion of Traditional Power Grid to Internet Energy IJEER 8(4), 37-40. DOI: <https://doi.org/10.37391/IJEER.080401>
- [17] S. Pal et al., "A Cascaded Nine-Level Inverter Topology with T-Type and H-Bridge With Increased DC-Bus Utilization", IEEE Transactions on Power Electronics, vol. 36, no. 1, pp. 285-294, 2021.
- [18] J. Kartick, B. Sujit and K. Suparna, "Dual reference phase shifted pulse width modulation technique for a N -level inverter based grid connected solar photovoltaic system", IET Renewable Power Generation, vol. 10, no. 7, pp. 928-935, 2016.
- [19] N. Sandeep and U. Yaragatti, "Operation and Control of an Improved Hybrid Nine-Level Inverter", IEEE Transactions on Industry Applications, vol. 53, no. 6, pp. 5676-5686, 2017.
- [20] B. Sharma, R. Dahiya and J. Nakka, "Effective grid connected power injection scheme using multilevel inverter based hybrid wind solar energy conversion system", Electric Power Systems Research, vol. 171, pp. 1-14, 2019.
- [21] P. Kala and S. Arora, "Implementation of Hybrid GSA SHE Technique in Hybrid Nine-Level Inverter Topology", IEEE Journal of Emerging and Selected Topics in Power Electronics, vol. 9, no. 1, pp. 1064-1074, 2021.
- [22] M. Braik, A. Hammouri, J. Atwan, M. Al-Betar and M. Awadallah, "White Shark Optimizer: A novel bio-inspired meta-heuristic algorithm for global optimization problems", Knowledge-Based Systems, vol. 243, p. 108457, 2022.
- [23] S. Jafarzadeh Ghouschi, S. Manjili, A. Mardani and M. Saraji, "An extended new approach for forecasting short-term wind power using modified fuzzy wavelet neural network: A case study in wind power plant", Energy, vol. 223, p. 120052, 2021.
- [24] P. Meenalochini and E. Sakthivel, "An efficient GBDTRSO control strategy for PV connected H-Bridge Nine Level MLI System with quasi-Z-source inverter", Applied Soft Computing, vol. 113, p. 108026, 2021.
- [25] Neha Tak; Sumit K Chattopadhyay Evaluation of High-Resolution Cascaded Multilevel Inverter Topologies for Renewable Energy Applications 2023 IEEE IAS Global Conference on Renewable Energy and Hydrogen Technologies (GlobConHT)



© 2023 by the Ch. Santosh Kumar and S. Tara Kalyani. Submitted for possible open access publication under the terms and conditions of the Creative Commons Attribution (CC BY) license (<http://creativecommons.org/licenses/by/4.0/>).